Proc. Indian Acad. Sci. (Earth Planet. Sci.), Vol. 97, No. 1, July 1988, pp. 53–62. © Printed in India.

# Seasonal cycle of surface circulation in the coastal North Indian Ocean

S R SHETYE and S SATHEESH CHANDRA SHENOI
National Institute of Oceanography, Dona Paula 403 004, India

MS received 13 November 1987; revised 23 May 1988

**Abstract.** Monthly-mean winds and currents have been used to identify the driving mechanisms of seasonal coastal circulation in the North Indian Ocean. The main conclusions are: (i) the surface circulation off Arabia is typical of a wind-driven system with similar patterns of longshore current and wind stress; (ii) circulation off the west coast of India is consistent with the dynamics of a wind-driven eastern boundary current only during the southwest monsoon. During the northeast monsoon it is possible that the influence of the interior flow is important. (iii) There are at least three mechanisms that influence the surface circulation off the east coast of India: wind-stress, influence of fresh-water run off and contribution of the interior flow. It is difficult at present to assess the relative importance of these three processes.

**Keywords.** Coastal currents; wind stress; Sverdrup transport; Munk layer; monsoons; North Indian Ocean.

## 1. Introduction

The North Indian Ocean is one of the few oceanic regimes that come under the influence of the annual cycle of the monsoonal winds. Under its influence, the coastal circulation in the region exhibits a well-marked seasonal cycle. This special feature has prompted study of the circulation off Somalia, where the annual cycle is the most pronounced (Schott 1983). Little is, however, known about the nature of the coastal circulation over the rest of the North Indian Ocean and still lesser about the causes behind it. In this note we examine this problem by looking at two sets of readily available maritime data: monthly-mean winds and monthly-mean surface currents. The latter are based on ship-drift values.

Our approach is similar to that used by Wooster *et al* (1976) to study the coastal circulation along the east coast of the N. Atlantic. Since the longshore component of the local wind stress ($\tau_l$) has been identified as one of the principal forcing function for the longshore coastal currents ($V_l$), we begin by comparing the annual cycles of $\tau_l$ and $V_l$. In the area where the two match, we conclude that the local winds dominate the surface coastal circulation. If they do not, we examine possible alternatives. As the circulation off Somalia has been a topic of considerable attention, this coast has not been included in the discussion. The rest of the coastline has been divided into three subareas—the Arabian Coast, the West Coast and the East Coast of India.

## 2. Seasonal variation of $\tau_l$ and $V_l$

The KNMI Atlas (1952) gives the monthly-mean ship-drift values on a two degree-grid over the Indian Ocean. Figures 1a, b based on the atlas, give the drifts for grids located

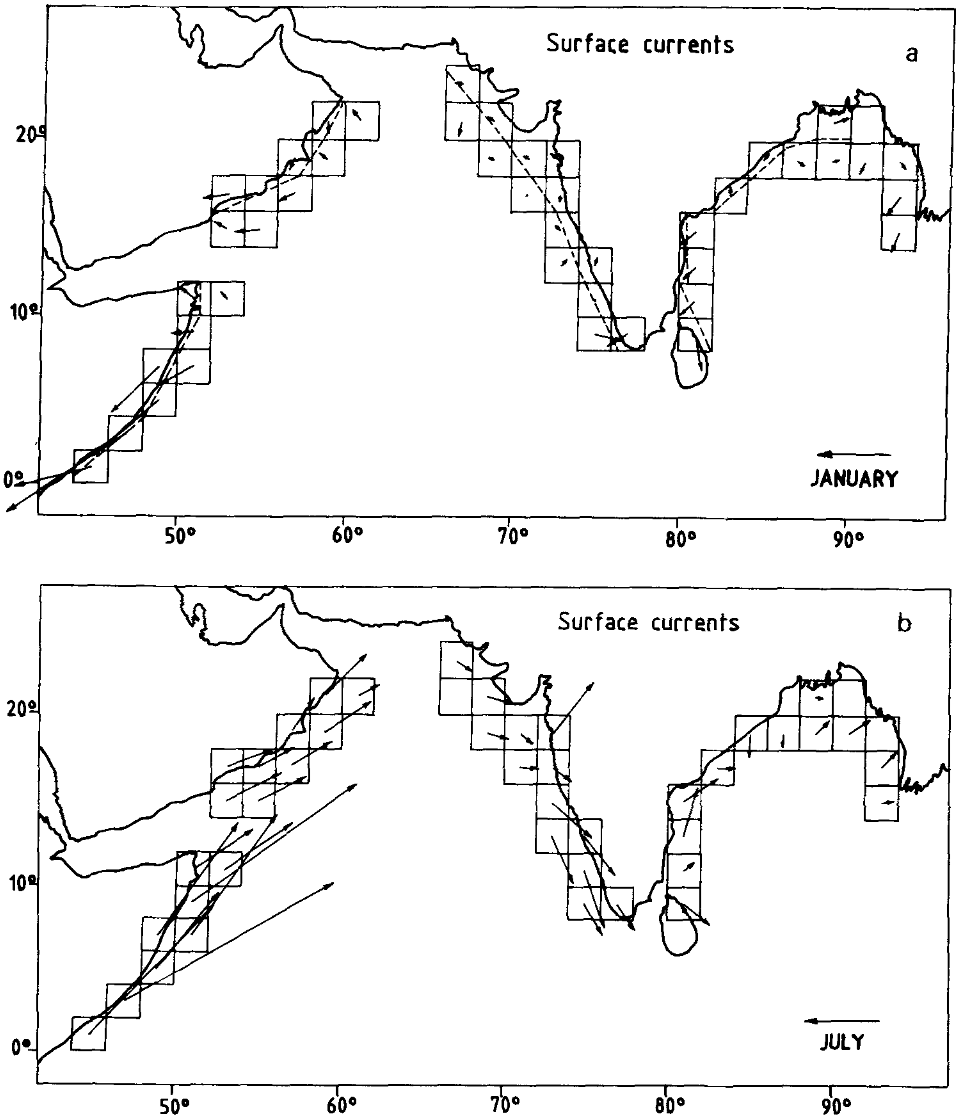


**Figure 1.** Monthly-mean ship drift in the North Indian Ocean based on KNMI Atlas (1952) for (**a**) January and (**b**) July. Arrow at the lower right hand corner of each figure has a magnitude of 50 cm/s.

in the North Indian coastal areas for January and July. The monthly mean longshore component of the surface currents has been computed by taking the component of the monthly-mean ship-drift along the straight line shown in each two-degree square in figure 1a. The 60-year climatology of monthly-mean resultant winds on a one-degree grid in the Indian Ocean has been given by Hastenrath and Lamb (1979). Using these data we first computed the monthly-mean wind for each grid in figure 1. These were then used to compute wind stress according to

$$\tau = \rho_a C_D W\mathbf{W},$$

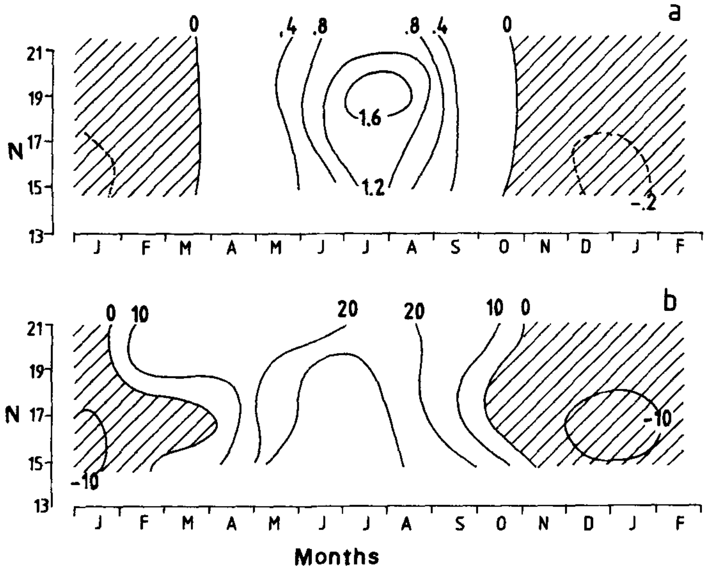


**Figure 2.** Monthly variation of longshore component of (**a**) wind stress $\tau_l$ (dyne/cm$^2$) and (**b**) surface velocity $V_l$ along the coast of Arabia. A positive value indicates that wind stress or velocity is pointed away from the equator.

where $\tau$ is the stress (Newton/m$^2$), $\rho_a$, the density of air (1·175 kg/m$^3$), $C_D$ an empirical drag coefficient taken to be $1{\cdot}3 \times 10^{-3}$, **W** the observed resultant wind and $W$ the speed. $\tau_l$ for a two-degree square was computed by taking the component of $\boldsymbol{\tau}$ along the line shown in each square of figure 1. Shetye *et al* (1985) used a similar procedure to define the annual cycle of monthly-mean wind stress in the coastal North Indian Ocean.

The first of the three subareas, the Arabian Coast, covers the coastline from 15 to 21°N. The second, the West Coast of India, covers the latitudes 9–23°N whereas the third, the East Coast of India, covers the region 9–21°N. The area east of 90° E has not been considered in the discussion. The sign convention is: $\tau_l$ is positive when the Ekman drift is offshore. This makes $\tau_l$ positive when poleward along a western boundary (i.e. coast of Arabia and the East Coast of India); $\tau_l$ is positive when equatorward along an eastern boundary (West Coast of India). The same sign convention is used for $v_l$.

As seen in figures 2a, b $\tau_l$ off the coast of Arabia is negative during November–March and positive during April–October. The behaviour of $V_l$ shows a similar pattern. In particular, reversals in $\tau_l$ and $V_l$ coincide. Earlier, Prell and Streeter (1982) pointed out that upwelling in this region is in phase with $\tau_l$.

Along the West Coast of India $\tau_l$ is positive (i.e. equatorward) throughout the year (figure 3a). $V_l$, on the other hand, is poleward between October and January (figure 3b). Hence, during the northeast (NE) monsoon the coastal current flows against the wind. During the rest of the year there is a fair resemblance between the two patterns.

The two patterns in figures 4a, b show some marked contrasts. $\tau_l$ is positive between March and October. $V_l$ on the other hand is positive between February and August. $V_l$ reverses direction in the middle of the southwest (SW) monsoon season when $\tau_l$ is close to its peak annual value. The reversal of the currents thus precedes the winds by a couple of months and occurs when the winds are at their strongest. $\tau_l$ shows a marked

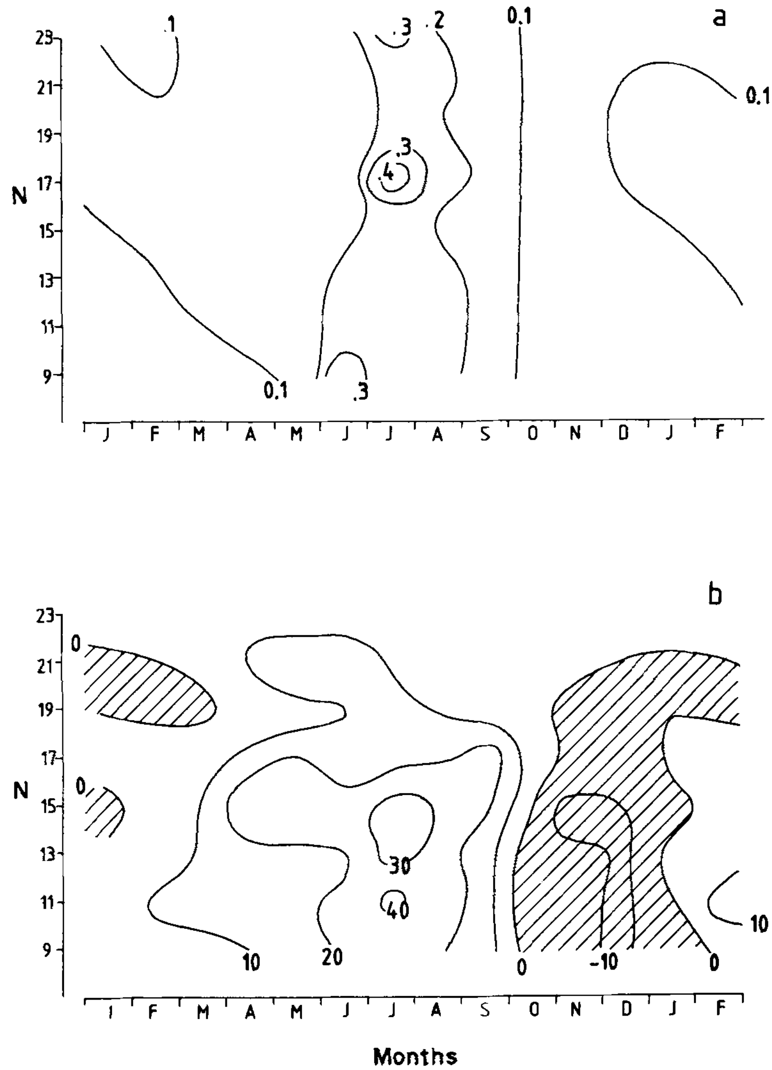


**Figure 3.** Monthly variation of longshore component of (**a**) wind stress $\tau_l$ (dyne/cm$^2$) and (**b**) surface velocity $V_l$ along the West Coast of India. A positive value indicates that wind stress or velocity is pointed towards the equator.

peak around 17 N in July, whereas the currents do not show any such behaviour. $V_l$ during August–January shows a systematic decrease in magnitude towards the north, a feature not seen in $\tau_l$ pattern. The reversal in the direction of $V_l$ around January precedes the reversal in winds by about a month.

## 3. Sverdrup transport in the North Indian Ocean

Currents along the western boundary of a basin are influenced by the interior Sverdrup flow. It is therefore worthwhile to examine the nature of the Sverdrup transport

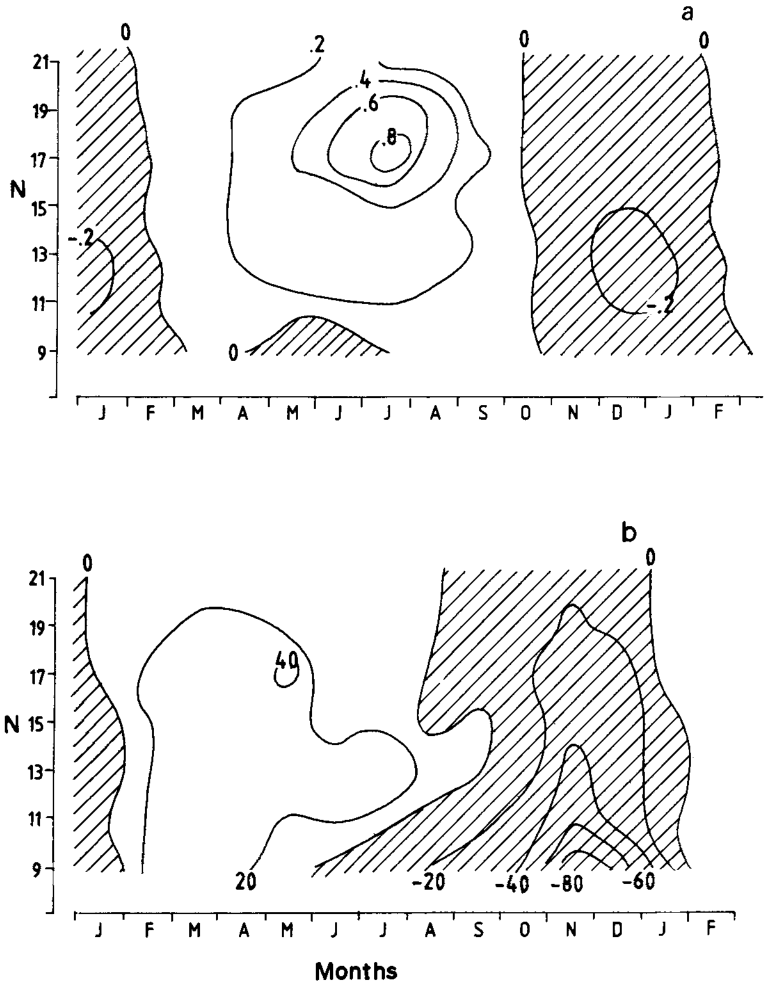


**Figure 4.** Same as figure 2, but for the East Coast of India.

streamfunction ($\psi$) given by

$$\partial\psi/\partial x = (1/\rho_0\beta)\,\mathrm{curl}\,\tau,$$

where $\tau$ is the wind stress, $\beta$ the rate of meridional variation of Coriolis parameter and $\rho_0$ the mean density of water (taken to be $1{\cdot}0\,\mathrm{g/cm^3}$). $\psi$ has been determined for two months: January, representative of the NE monsoon and July, representative of the SW monsoon. The curl of the wind stress given by Hastenrath and Lamb (1979) has been used except for one change. Hastenrath and Lamb (1979) use $2{\cdot}8 \times 10^{-3}$ for the value of the drag coefficient $C_D$. This value is more than twice the usual norm of approximately $1{\cdot}3 \times 10^{-3}$. The value of curl used in our computation has therefore been obtained after multiplying by 0·46 the value given by Hastenrath and Lamb. The computed $\psi$ is shown in figures 5a, b. A Munk layer is needed along the western boundary to close the circulation depicted in these figures. The strength of such a layer would be about 15 Sv transporting mass northward along the coast of Somalia in July and approximately

2 Sv southward in January. Along the coast of Arabia the contribution to Munk layer in January is negligible and it is of the order of 6 Sv equatorward in July. In the Bay of Bengal the contribution of the Munk layer is important only between 15° and 20°N, the magnitude and the direction of the flow being 3 Sv equatorward in July and 3 Sv poleward in January.

Bruce (1983) earlier computed the Sverdrup transport for the Arabian Sea. The pattern of transport given there agrees well with ours; however, the magnitudes are higher than ours because of the lower value of $C_D$ used in our computations.

## 4. Discussion

The general agreement between $\tau_l$ and $V_l$ patterns off Arabia suggests that the surface circulation off Arabia is driven primarily by the local winds. This observation is consistent with that of Prell and Streeter (1982) who concluded that the monthly mean upwelling in the region is controlled by $\tau_l$. Hence, the Arabian coastal circulation appears similar to the classical wind-driven circulation along the eastern boundaries. But, we have the implication of figure 5b that there has to be a southward flow of approximately 8 Sv in the Munk layer along this coast. Bruce (1983) also observed a similar disagreement between the Sverdrup transports computed from wind stress and the near surface transport computed from hydrographic observations. To reconcile with these apparently contrasting views we need to hypothesize the following structure for the flow: an "eastern-boundary-like" flow confined near the surface and controlled by local $\tau_l$ alone; and a deeper flow arising due to a Munk layer. The magnitude of the latter is controlled by the curl of wind stress east of the coast.

Off the west coast of India during the SW monsoon, when $\tau_l$ is at its peak, there is fair resemblance between the patterns of $\tau_l$ and $V_l$. Hence we conclude that during this season it is $\tau_l$ that primarily controls $V_l$. During November–January the surface current flows against $\tau_l$. This has also been pointed out by Pankajakshan and Rama Raju (1987). During this season the coastal current moves with the coastal pressure gradient (see charts 364 and 369 from Wyrtki (1971)). This is in contrast to the behaviour generally attributed to a wind-driven eastern boundary current. The poleward flow along the West Coast of India appears when $\tau_l$ is at its weakest, and hence it is safe to conclude that it is not forced by the latter.

A mechanism that has been suggested earlier to explain this current during November-January is the thermohaline forcing due to the poleward increase of surface density (Shetye 1984). Godfrey and Ridgeway (1985) pointed out that the poleward flowing Leeuwin current off the coast of West Australia, flows against $\tau_l$ and with the longshore surface pressure gradient. McCreary *et al* (1986) showed that the Leeuwin current can be driven by the alongshore poleward density increase arising due to the poleward temperature decrease in the interior regime off the West Coast of Australia. Such a density decrease is of course a manifestation of the large scale interior circulation off the Australian coast.

The magnitude of the alongshore density gradient off the West Coast of India varies seasonally, but always increases towards the north. The change in $\sigma_t$ from 10°N to 20°N is approximately $1{\cdot}1\ \mathrm{g/cm^3}$ in January–February, it reduces to 0·12 in July–August and is at its annual peak ($1.4\ \mathrm{g/cm^3}$) during November–December. Hence the density gradient is the strongest when $\tau_l$ is the weakest. Note that the change in

$\sigma_t$ from 25 to 35°S off the West Coast of Australia is approximately 1·4 g/cm$^3$ producing a density gradient of approximately $1{\cdot}3 \times 10^{-11}$ g/cm$^4$ and is constant throughout the year. $\tau_l$ along this coast has a maximum of 1 dyne/cm$^2$ in November–January and vanishes in June.

In short, the annual cycle of the surface current along the West Coast of India appears to be controlled by two opposing forcing functions: $\tau_l$ which tends to drive the surface flow towards the equator; and, longshore density gradient which tends to drive the current poleward. $\tau_l$ dominates during the SW monsoon season whereas the density gradient dominates during the NE monsoon season.

The coastal density gradient along the west coast arises mainly due to variation in salinity (see charts 38–57 in Wyrtki (1971)). This is in contrast to conditions generally observed elsewhere in the world (West Coast of Australia, for example) where the density gradient is normally due to temperature variation. The northern end of the Arabian Sea is connected to the Persian Gulf. The salinity in this mediterranean basin ranges between 37 and 41 ppt. Salinities higher than 36 ppt observed towards the northern end of the West Coast of India can be attributed to the presence of the Persian Gulf. Salinity near the southern end of the west coast ranges between 33 and 34 ppt and is typical of the low salinity waters of the eastern North Indian Ocean. The west coast thus lies at the interface between these two waters with marked salinity differences.

There are two major differences between the $\tau_l$ and $V_l$ patterns brought out by figures 4a and b. The first of these is the absence of a "cell-like" maximum at approximately 17°N around July in the $\tau_l$ pattern. The second is that the distinct increase in $V_l$ towards the southern end of the East Coast of India is not seen in the $\tau_l$ pattern. As seen below there are two possible explanations for these differences: contribution of the Sverdrup flow, and the influence of freshwater run off on the coastal currents.

The Sverdrup flow in the Bay of Bengal during July and January is shown in figure 5. The wind stress curl over the northern bay is positive during July. The resulting Munk layer along the coast of India would therefore be required to transport about 3 Sv southward. During January the wind stress curl is negative. The expected transport is 3 Sv northward. At present it is not known to what extent the Munk transport influences the surface flow along the East Coast. However, it is a potential candidate to explain the absence of the maximum in $V_l$ observed at 17°N around July.

The importance of freshwater run off as a driving mechanism for coastal currents has been highlighted by Royer (1979). Royer (1982) pointed out that the precipitation in the coastal mountains of the northeast Pacific produces a freshwater discharge with an annual average of 23,000 m$^3$/s. The water enters the sea by way of numerous small rivers and streams, forming a "line-source" of low density water. The freshwater creates a cross shelf density gradient that drives a longshore geostrophic baroclinic jet moving with the land to the right of it. Royer (1982) estimated that the width of the jet is less than 25 km, and has speeds in excess of 100 cm/s, and transport in excess of $1{\cdot}3 \times 10^6$ m$^3$/s. It was also suggested that the flow is maintained as a narrow current adjacent to the coast by the wind stress that causes downwelling conditions.

The Bay of Bengal is a region which experiences evaporative loss varying from 3 to 6 mm water/day (Hastenrath and Lamb 1979). The bay, however, receives considerable freshwater as run off from the rivers that border it and from the atmosphere through precipitation. Prominent amongst the rivers are the Brahmaputra and the Ganga. Bumgartner and Reichel (1975) estimated that the annual mean run off of the Brahmaputra into the Bay of Bengal is 20,000 m$^3$/s, and that of Ganga is 15,500 m$^3$/s. A

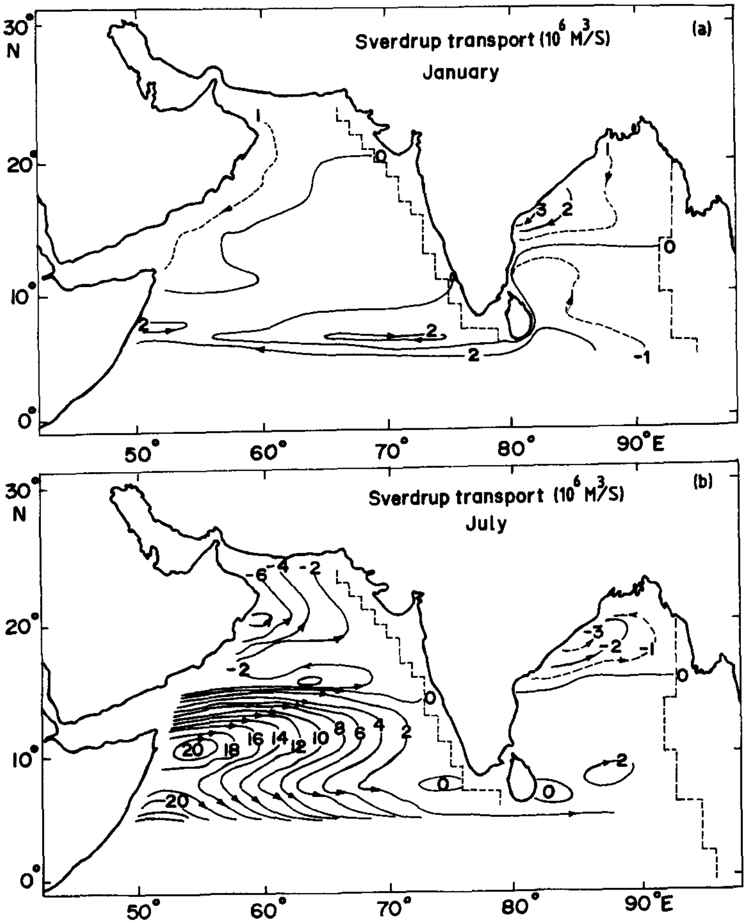


**Figure 5.** Sverdrup transport: $\psi$ ($10^6\,m^3/s$) in the North. Indian Ocean north of 5°N in (**a**) January and (**b**) July. The dashed line in the figure gives the 'eastern boundary' where $\psi$ has been set to zero.

large fraction of this run off occurs during the four months of the SW monsoon season. In addition to these rivers there are others which discharge freshwater along the East Coast of India. These include the Mahanadi, the Godavari, the Krishna and the Cauvery. Figures on freshwater contribution of these rivers to the Bay are not available. It is known, however, that the peak discharge in Mahanadi, Godavari and Krishna generally occurs during August. The mean discharge during this month at gauging station Kaimundi on Mahanadi has been reported to be $7710\,m^3/s$ (Anon 1969). The corresponding figures at Dowlaishwaram on Godavari and at Vijayawada on Krishna are $11{,}900\,m^3/s$ and $6{,}550\,m^3/s$ (Anon 1969). Towards the southern end of the east coast peak rainfall occurs later, generally in November. The peak discharge at Vellore on Pennar occurs in November (Anon 1969). Rao (1979) reported that the mean annual flow in Cauvery basin is $6{,}600\,m^3/s$.

On the whole, despite the uncertainties in the present estimates of freshwater run off, it is safe to assume that the total freshwater run off along the East Coast of India is well in excess of 30,000 $m^3$, and that a large fraction of this occurs during the four months of the SW monsoon. Comparing this figure with that for the Alaska coast, it appears that the coastal freshwater input is a strong candidate for driving the coastal circulation. It is possible that the freshwater run off is related to the differences between the $\tau_l$ and $V_l$ patterns that were pointed out earlier. During the SW monsoon the freshwater run off is at a peak in the northern part of the coast. This can set up a cross-shore salinity and density gradient. The resulting baroclinic pressure gradient would tend to drive an equatorward geostrophic flow along the coast, opposing the poleward current that $\tau_l$ could set up. The hydrographic observations (Gopalakrishna and Sastry 1985) do show a cross-shore density gradient resulting from the increasing salinities away from the coast. During the NE monsoon the freshwater influx increases towards the southern end. This could drive an equatorward baroclinic current whose magnitude would increase towards the south, because the freshwater influx is higher there. $\tau_l$ at this time is equatorward. The winds would therefore tend to converge the freshwater near the coast, creating a situation similar to the one off Alaska.

## 5. Conclusions

(i) The surface circulation off the coast of Arabia is typical of a wind-driven coastal current, with $\tau_l$ and $V_l$ exhibiting similar patterns.

(ii) Circulation off the West Coast of India is consistent with the dynamics of a wind-driven eastern boundary current only during the SW monsoon. During the NE monsoon it is possible that the influence of the interior flow as envisioned by McCreary *et al* (1986) is important.

(iii) There appears to be at least three competing mechanisms that influence the surface circulation off the East Coast of India: wind-stress, influence of freshwater run off and contribution of a Munk layer driven by Sverdrup flow. It is not possible at present to assess the relative importance of these three processes.

One of the primary objectives behind undertaking this study was to generate hypotheses regarding the dynamics of coastal circulation in the North Indian Ocean, more importantly along the coast of India, so that future studies can be aimed at testing these hypotheses. In view of this, it is worthwhile to list some of the specific questions which need to be addressed: (a) During the NE monsoon, is the interior circulation in the Arabian Sea consistent with that necessary to drive the eastern boundary current according to the mechanism outlined by McCreary *et al* (1986)? (b) What are the spatial and temporal variations of the freshwater run off along the coasts of India? (c) It would also be worthwhile to examine the dynamics of coastal currents that are driven by both wind and freshwater influx.

## References

Anonymous 1969 Discharge of selected rivers of the world, UNESCO, Paris

Bruce J C 1983 The wind field in the Western Indian Ocean and the related ocean circulation; *Mon. Weather Rev.* **111** 1442–1452

Bümgartner A and Reichel E 1975 *The world water balance mean annual global, continental and maritime precipitation evaporation and run off,* (Amsterdam; Elsevier) p. 179

Godfrey J S and Ridgeway K R 1985 The large-scale environment of the poleward-flowing Leeuwin current, Western Australia: longshore steric height gradients, wind stresses and geostrophic flow; *J. Phys. Oceanogr.* **15** 481–495

Gopalakrishna V V and Sastry J S 1985 Surface circulation over the shelf off the East Coast of India during the southwest monsoon; *Indian J. Mar. Sci.* **14** 62–65

Hastenrath S and Lamb P J 1979 *Climatic atlas of the Indian Ocean, Parts 1 and 2: Surface climate and atmospheric circulation,* (Madison: Wisconsin University Press)

KNMI (Koninklijk Nederlands Meteorolgisch Institut) 1952 *Indische ocean oceanographische en meteorologische gegevens,* 2 edn. Publication No. 135

McCreary J P, Shetye S R and Kundu P K 1986 Thermohaline forcing of eastern boundary currents: With application to the circulation off the west coast of Australia; *J. Mar. Res.* **44** 71–92

Pankajakshan T and Rama Raju D V 1987 Intrusion of Bay of Bengal water into Arabian Sea along the West Coast of India during northeast monsoon. *Contribution in marine sciences. Dr S Z Quasim Sastyabdapurthi felicitation volume* (eds) T S S Rao, R Natarajan, B N Desai, G N Swami and S R Bhat (Dona-Paula, Goa: National Institute of Oceanography) p. 237–244

Prell W L and Streeter H F 1982 Temporal and spatial patterns of monsoonal upwelling along Arabia: A modern analogue for the interpretation of quarternary SST anomalies; *J. Mar. Res.* **40** 143–155

Rao K L 1979 *India's water wealth: Its assessment uses and projection* (New Delhi Orient Longmans) p. 267

Royer T C 1979 On the effect of precipitation and run off on coastal circulation in theGulf of Alaska; *J. Phys. Oceanogr.* **9** 71–79

Royer T C 1982 Coastal freshwater discharge in the northeast Pacific; *J. Geophys. Res.* **87** 2017–2021

Schott F 1983 Monsoon response of the Somali current and associated upwelling, in *Progress in oceanography* (eds) M V Angel and J O' Brien (New York: Pergamon Press) vol. 12, pp. 357–382

Shetye S R 1984 Seasonal variability of the temperature field off the southwest coast of India; *Proc. Indian Acad. Sci.* (*Earth Planet. Sci.*) **93** 399–411

Shetye S R, Shenoi S S C, Antony M K and Kumar V K 1985 Monthly-mean wind stress along the coast of the North Indian Ocean, *Proc. Indian Acad. Sci.* (*Earth Planet. Sci.*) **94** 129–137

Wooster W, Bakun A and Mc Lain D 1976 The seasonal upwelling cycle along the eastern boundary of the North Atlantic; *J. Mar. Res.* **34** 131–141

Wyrtki K 1971 *Oceanographic atlas of the International Indian Ocean expedition,* National Science Foundation, US (Washington DC: Government Printing Office)